Biomaterials 30 (2009) 5877–5884

Contents lists available at ScienceDirect

Biomaterials

journal homepage: www.elsevier.com/locate/biomaterials

Mixed-mode fracture of human cortical bone

Elizabeth A. Zimmermann [a,b], Maximilien E. Launey [a], Holly D. Barth [a,b,c], Robert O. Ritchie [a,b,*]

[a] Materials Sciences Division, Lawrence Berkeley National Laboratory, Berkeley, CA 94720, USA
[b] Department of Materials Science and Engineering, University of California, Berkeley, CA 94720, USA
[c] Experimental Systems Group, Lawrence Berkeley National Laboratory, Berkeley, CA 94720, USA

ARTICLE INFO

Article history:
Received 28 May 2009
Accepted 10 June 2009
Available online 1 July 2009

Keywords:
Human cortical bone
Mixed-mode fracture
Fracture toughness
Fracture mechanisms

ABSTRACT

Although the mode I (tensile opening) fracture toughness has been the focus of most fracture mechanics studies of human cortical bone, bones *in vivo* are invariably loaded multiaxially. Consequently, an understanding of mixed-mode fracture is necessary to determine whether a mode I fracture toughness test provides the appropriate information to accurately quantify fracture risk. In this study, we examine the mixed-mode fracture of human cortical bone by characterizing the crack-initiation fracture toughness in the transverse (breaking) orientation under combined mode I (tensile opening) plus mode II (shear) loading using samples loaded in symmetric and asymmetric four-point bending. Whereas in most structural materials, the fracture toughness is *increased* with increasing mode-mixity (i.e., where the shear loading component gets larger), in the transverse orientation of bone the situation is quite different. Indeed, the competition between the maximum applied mechanical mixed-mode driving force and the weakest microstructural paths in bone results in a behavior that is distinctly different to most homogeneous brittle materials. Specifically, in this orientation, the fracture toughness of bone is markedly *decreased* with increasing mode-mixity.

Published by Elsevier Ltd.

1. Introduction

Most fracture mechanics based studies concerning the fracture resistance, or toughness, of materials have been performed under nominally uniaxial, principally tensile, loading conditions. This is mainly because, in the presence of a crack, the fracture toughness under such mode I (tensile opening) loading is invariably the worst-case, i.e., the toughness in mode I is lower than under mixed-mode or mode II loading[1]. Fracture mechanics studies on human cortical bone are no exception here with the vast majority of research being focused on the mode I fracture toughness[2]. Although such research has generally been illuminating with respect to the nano/micro-structural origins of fracture resistance in bone [1–4], specifically for discerning the salient toughening mechanisms involved, physiologically bone is rarely loaded solely in this manner. Most cracks that are formed in bone are loaded under mixed-mode conditions created either by the shape of the bone, the nature of the *in vivo* loads and/or the orientation of cracks with respect to these loads. Due to the anisotropy of human cortical bone and the presence of such multiaxial loading, it cannot be presumed that a crack will propagate in mode I nor whether the measured toughness values and microstructural toughening mechanisms, which have been identified in laboratory samples invariably loaded in mode I, have any relevance to *in vivo* conditions. Moreover, it has not been established for all orientations that the mode I fracture toughness is really the worst-case in a material such as bone.

In fracture mechanics terms, when a crack is loaded under mixed-mode conditions (Fig. 1), the crack-driving force can be described in terms of the critical strain energy release rate, G, which can be defined in terms of the applied stress intensities, K_I, K_{II} and K_{III}, by the following expression [5]:

$$G = K_I^2/E' + K_{II}^2/E' + K_{III}^2/2\mu, \quad (1)$$

where μ is the shear modulus and E' is the Young's modulus, E, in plane stress and $E/(1-\nu^2)$ in plane strain (where ν is Poisson's ratio). For combined modes I and II loading, the mode-mixity of the applied driving force, i.e., the relative proportion of K_{II} to K_I can be described by the so-called phase angle, Ψ, which is defined as:

* Corresponding author. Department of Materials Science and Engineering, University of California, 216 Hearst Mining Bldg., MC 1760, Berkeley, CA 94720, USA. Tel.: +1 510 486 5798; fax: +1 510 643 5792.
E-mail address: roritchie@lbl.gov (R.O. Ritchie).

[1] In certain situations, there can be an additional out-of-plane shear loading component in mode III (anti-plane shear).

[2] The fracture toughness, K_{ic},(where i = I, II or III) is the critical value of the stress intensity K for unstable fracture in the presence of a pre-existing crack, i.e., in mode I when $K = Y\sigma_{app}(\pi a)^{1/2} = K_{Ic}$, where σ_{app} is the applied stress, a is the crack length, and Y is a function (of order unity) of crack size and geometry. Alternatively, the toughness can be expressed as a critical value of the strain energy release rate, G_c, defined as the change in potential energy per unit increase in crack area.

0142-9612/$ – see front matter Published by Elsevier Ltd.
doi:10.1016/j.biomaterials.2009.06.017

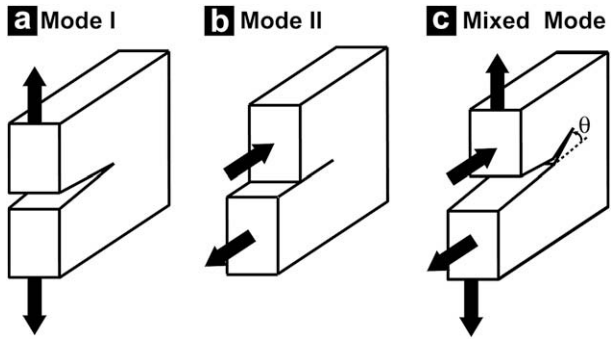

Fig. 1. Schematic illustrating the different modes of loading: (a) mode I (tensile loading), (b) mode II (shear loading) and (c) mixed-mode. Mixed-mode loading is a superposition of mode I and mode II stress intensities that creates a mixed-mode driving force at the crack tip that causes the crack to grow at an angle, θ, to the original crack plane.

$$\Psi = \tan^{-1}\left[\frac{K_{II}}{K_I}\right], \tag{2}$$

such that the phase angles for pure mode I and pure mode II loading are, respectively, 0° and 90°.

In the presence of a crack, the application of mixed-mode loading creates both tensile (mode I) and shear (mode II) driving forces at the crack tip that invariably results in directional changes in the crack path. For this reason, the crack path trajectory has been used as a primary indicator of the underlying material behavior and has traditionally been used, along with the applied stress intensities, to formulate mixed-mode fracture criteria [6–8]. The application of pure mode I loading generates a maximum tensile driving force ahead of the crack tip, which results in coplanar crack growth; similarly, the application of pure mode II loading generates a maximum shear driving force ahead of the crack tip. However, under pure mode II conditions most materials do not exhibit coplanar crack growth [9]; instead, the crack invariably kinks at some angle, θ (Fig. 1c). Similarly, a mixed-mode driving force (modes I and II) also leads to crack kinking (and to crack twisting if a mode III anti-plane shear component is involved). Various fracture criteria have been developed to predict fracture and angle of crack growth; the vast majority are based solely on the mechanical notion (and direction) of a maximum mixed-mode driving force, and pertain principally to ideally brittle materials. Two such criteria considered here are the maximum strain energy release rate criterion, G_{max}, and the $K_{II} = 0$ criterion. The G_{max} criterion assumes that the crack trajectory will follow the path along which the strain energy release rate is maximum, while the $K_{II} = 0$ criterion assumes that the crack will grow along the direction where the mode I stress intensity is at a maximum. In the literature, these two principal criteria have been used to numerically compute the direction of crack growth as a function of the phase angle in a homogeneous material [10]. Both the $K_{II} = 0$ criterion and the G_{max} criterion predict virtually identical crack paths and only differ slightly at very large phase angles. However, it must be noted that they both rely solely on a mechanical description of the crack-driving force – they make no consideration for the presence of microstructural anisotropy in the material under test, e.g., to the presence of "weak" microstructural paths; moreover, by focusing on tensile-stress dominated criteria, they are largely applicable to nominally brittle materials.

Like bone, many structural components experience mixed-mode loading while in use, where it is presumed that the toughness, G_c, is lowest in mode I and increases monotonically with an increasing mode II component, as shown for a variety of materials in Fig. 2. As noted above, models for this behavior center on the notion of a maximum driving force, e.g., G_{max}. It has been suggested that the

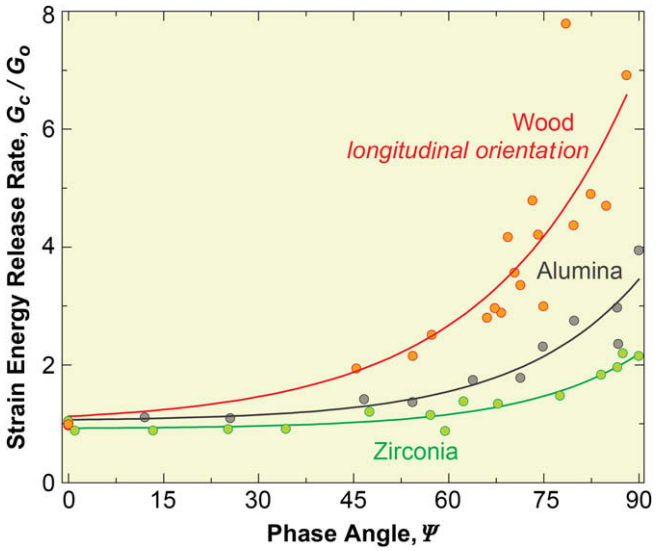

Fig. 2. The typical relationship between the critical strain energy release rate, G_c, and the phase angle, Ψ, for a variety of materials, namely wood (in its longitudinal direction) [29], alumina [7], and zirconia [7]. For comparison, G_c is here normalized by the lower-bound toughness, G_o. The toughness is lowest in mode I, at $\Psi = 0°$, and increases monotonically with the relative proportion of the mode II shear component until reaching a maximum under mode II conditions, at $\Psi = 90°$.

strain energy accumulates, at higher phase angles, in part due to crack surface interferences, e.g., those associated with frictional sliding, abrasion and even locking of asperities between the mating crack surfaces [11–13]. However, such mechanical driving force considerations strictly pertain to homogeneous, brittle materials where the crack follows a G_{max} or $K_{II} = 0$ path. In anisotropic materials, the crack trajectory, and hence the fracture toughness, result from the competition between the path of maximum mechanical driving force and the path of "weakest resistance" in the microstructure.

Where these two directions are commensurate, predictions based solely on the maximum driving force criteria remain valid. Where they are incommensurate, complex crack path configurations often result, leading to significant crack deflections and twists; such deviations from the direction of maximum driving force act to "shield" the crack from the applied stresses/strains, i.e., they lower the effective (local) stress intensity actually experienced at the crack tip, resulting in higher toughness [14]. As we show in this work, human cortical bone fractured in the transverse (breaking) orientation fits exactly into this latter category with the path of maximum driving force in mode I being essentially orthogonal to the preferred microstructural paths.

2. Background

Complex cracking configurations in bone result from the hierarchical and directional nature of its structure. Bone is a composite of collagen and hydroxyapatite (HA), with characteristic structural features over innumerable length-scales. These include twisted peptide chains at the nanoscale, HA-impregnated twisted collagen fibrils at the scale of tens of nanometers, micrometer-diameter collagen fibers arranged in various lamellar structures at micrometer dimensions, and (secondary) osteon (Haversian) structures at the scale of several hundred micrometers in size. The latter Haversian systems are particularly important to bone fracture; they comprise a central neurovascular cavity, roughly 50–90 μm in diameter, surrounded by concentric lamellae (3–7 μm thick) of collagen fibrils and mineral [15]. The interfaces that separate the

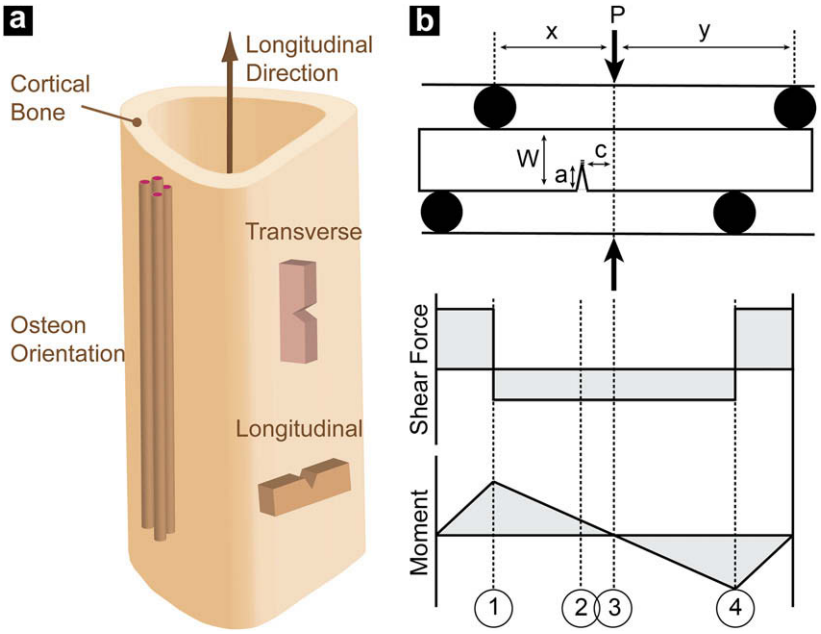

Fig. 3. Schematic (a) shows the structure of human bone as well as the two anatomical orientations (transverse and longitudinal) of the test samples. (b) The single-edge notched specimens were tested using an asymmetric four-point bend rig. The load is applied through the center line of the rig, which creates, through the mid-span of the sample, a constant shear force and a linearly varying bending moment. Vertical lines 1 and 4 represent the location of the inner loading pins. When the crack is aligned with the centerline of the rig, line 3, only a shear force is applied, which creates a mode II driving force. When the crack is offset from the centerline of the rig, for example line 2, a shear force and a moment are applied which creates a mixed-mode driving force. Thus, the phase angle, defined as $\Psi = \tan^{-1}(K_{II}/K_I)$, is a function of the offset of the crack, c, from the centerline.

Haversian lamellae from the interstitial lamellae [16,17], the so-called cement lines or sheaths (these regions contain less collagen and are laid down prior to lamellae deposition during bone remodeling [16,17]), represent especially weak regions which can act as sites where major microcracks form. In contrast to earlier claims [18,19], Skedros et al. [20] have shown recently that cement lines are highly mineralized, which is almost certainly why microcracks form preferentially there. Since the cement lines are aligned nominally in the longitudinal direction of the bone, they are critical to the fracture trajectories in bone and hence to the resultant toughness.

There have been only a few prior studies on the toughness of bone under mixed-mode loading. In one study, the mode II toughness of human cortical bone was found to be greater than the mode I toughness by a factor of ~3 in the longitudinal direction [21]; no results were obtained for other orientations[3]. Another study compared the mode I and mode II fracture toughness of bovine cortical bone in the longitudinal and transverse directions and again found the usual result that the mode I fracture toughness was the lower-bound [22]. However, in this latter study, the authors side-grooved their samples by as much as 50% of their original thickness; this has the effect of forcing the crack to take an (unnatural) coplanar path by suppressing the extrinsic mechanisms which deflect the crack, resulting in an artificial result.

In light of such limited results for the fracture toughness behavior of bone under multiaxial loading conditions, the objective of the present study is to characterize the mixed-mode crack-initiation fracture toughness of human cortical bone as a function of the phase angle (i.e., in terms of the relative proportion of the K_{II} to K_I components). Experiments are focused on the transverse (breaking) and the longitudinal (splitting) orientation and are interpreted mechanistically in terms of the mutual competition between the preferred crack path directions dictated by the mechanical driving force and the microstructural resistance.

3. Experimental methods

3.1. Materials

Fresh frozen human cadaveric femurs, from three males aged 48, 52, and 79 years of age with no known metabolic bone diseases, were used in this study (which was exempt from human subjects authorization because no identifying information was known about the donors). A total of 25 samples were tested using a notched asymmetric four-point bending test to determine the mixed-mode toughness: $N = 7$ from the 48-year-old donor, $N = 11$ from the 52-year-old donor, and $N = 7$ from the 79-year-old donor. The cortical bone, taken from the diaphysis of each femur, was sectioned with an IsoMet 1000 precision low-speed saw (Buehler) into rectangular cross-sectioned beams with width $W \sim 3.3$–4.9 mm and thickness $B \sim 2.0$–3.0 mm. The samples were notched with a low-speed saw in the transverse (breaking) orientation; in this orientation, the notch is oriented such that the nominal crack growth direction is from the periosteum to the endosteum and perpendicular to the long axis of the osteons (*out-of-plane* transverse), as shown in Fig. 3a. The notches were sharpened by polishing at the root of the notch with a razor blade, which was irrigated with 1 μm diamond suspension, to give a final crack length of $a \sim 1.3$–2.6 mm. As a basis for comparison, four additional samples of human cortical bone from a 50-year-old male donor were tested in the longitudinal orientation. In these samples, the orientation of the notch was such that the nominal crack growth direction was along the proximal–distal direction that is parallel to the long axis of the osteons (*in-plane* longitudinal), as shown in Fig. 3a. All samples were ground with successively finer grit to a 1200 grit finish prior to a final polishing with a 1 μm and then a 0.05 μm diamond suspension. They were stored in Hanks' Balanced Salt Solution (HBSS) for at least 12 h prior to testing.

3.2. Fracture toughness measurements

In order to measure the fracture toughness while simultaneously imaging the initiation and growth of cracks in real time, *in situ* testing of samples soaked in HBSS was performed in a Hitachi S-4300SE/N environmental scanning electron microscope (ESEM) (Hitachi America, Pleasanton, CA) at 25 °C using a Gatan Microtest 2kN four-point bending stage (Gatan, Abington, UK); images of the crack path were obtained simultaneously in back-scattering electron mode at a voltage of 25 kV and a pressure of 35 Pa. Loading was applied under displacement control at a displacement rate of 6.67 μm/s, with an in-house machined rig to apply an asymmetric or

[3] For definition of the transverse and longitudinal orientations with respect to the long axis of the bone (and hence the nominal direction of the osteons), see Fig. 3a.

symmetric four-point bending load to the sample. The value of the critical fracture toughness, G_c, was defined after a crack extension of 100 μm. This arbitrary criteria guaranteed through-thickness cracking in all the tests, and no crack growth at locations other than the crack tip (e.g., at the loading pins).

Whereas a pure mode I loading configuration ($\Psi = 0^\circ$) was achieved using symmetrical four-point bending (pure bending), pure mode II loading ($\Psi = 90^\circ$) and various degrees of mixed-mode (mode I + II) loading were obtained with similar notched bend specimens loaded asymmetrically. The asymmetric four-point bending configuration applies a constant shear force, Q, to the crack tip and a moment, M, whose magnitude varies linearly with displacement, c, from the center line of the rig (Fig. 3b). Accordingly, the phase angle can be tuned by varying the position of the crack with respect to the center line of the rig, which results in a shear force and bending moment (both per unit thickness) at the crack tip:

$$Q = P\frac{y-x}{y+x} \text{ and } M = cQ, \tag{3}$$

where P is the applied load, and y and x are the larger and smaller loading spans, respectively, of the rig at which point the load is applied to the sample (Fig. 3b). For the asymmetric specimen geometry, He and Hutchinson [23] give the most recent linear-elastic stress intensity factor solution for K_I and K_{II} in terms of the crack length, a, and the specimen width, W, as:

$$K_I = \frac{6M}{W^2}\sqrt{\pi a}F_I\left(\frac{a}{W}\right) \text{ and } K_{II} = \frac{Q}{W^{\frac{1}{2}}}\frac{(a/W)^{\frac{3}{2}}}{(1-a/W)^{\frac{1}{2}}}F_{II}\left(\frac{a}{W}\right), \tag{4}$$

where F_I and F_{II}, are the geometry functions tabulated, respectively, by Tada [24] and He and Hutchinson [23], and are expressed as:

$$F_I\left(\frac{a}{W}\right) = \frac{6\sqrt{2\tan\left(\frac{\pi a}{2W}\right)}}{\cos\left(\frac{\pi a}{2W}\right)}\left[0.923 + 0.199\left\{1-\sin\left(\frac{\pi a}{2W}\right)\right\}^4\right],$$

$$F_{II}\left(\frac{a}{W}\right) = 7.264 - 9.37\left(\frac{a}{W}\right) + 2.74\left(\frac{a}{W}\right)^2 + 1.87\left(\frac{a}{W}\right)^3 - 1.04\left(\frac{a}{W}\right)^4. \tag{5}$$

As noted above, the mode I fracture toughness was measured on single-edge notched bend samples loaded in symmetric four-point bending. The loading configuration creates a region of constant moment between the inner two loading points. Thus, the stress intensity factor solution can be obtained for an edge-cracked plate in pure bending [25], which is equivalent to the solution for K_I in asymmetric loading Eq. (4), only with a moment of $M = P(S_2 - S_1)/4$, where S_2 and S_1 are respectively, the major and minor loading spans.

The longitudinal samples were tested in asymmetric three- and four-point bend [23,26], and in symmetric four-point bend. No crack growth was observed prior to sample failure at locations other than the crack tip. Consequently, these tests must be considered to be yielding a lower-bound for the value of the fracture toughness.

3.3. X-ray computed tomography

Micro X-ray computed tomography (μXCT) is a nondestructive characterization technique that was employed to visualize the three-dimensional mixed-mode crack path of transversely-loaded human cortical bone. The X-ray micro-tomography was performed at the Advanced Light Source synchrotron radiation facility at Lawrence Berkeley National Laboratory. Tomographic images were taken of two samples after roughly 500 μm of crack growth under either mode I or mode II loading conditions, as previously described.

The μXCT setup is similar to the standard setup for this technique [27] whereby samples are rotated (through a 180° angle) in a monochromatic X-ray beam of 20 KeV, which was chosen in order to maximize the signal to noise ratio. During each 180° rotation, two-dimensional images were taken every 0.25° for the mode I sample and every 0.15° for the mode II sample. The transmitted X-rays were imaged via a scintillator, magnifying lens and a digital camera yielding an effective voxel size in the reconstructed three-dimensional image of 1.8 μm. The samples were scanned in absorption mode and the reconstructed images were obtained using a filtered back projection algorithm. In absorption mode, the gray scale values of the reconstructed image are representative of the absorption coefficient. The data sets were reconstructed using the Octopus software [28] and the three-dimensional visualization was performed using Avizo (Mercury Computer Systems, Inc.).

4. Results

Results showing the variation in the fracture toughness of human cortical bone (defined in terms of the critical value of the strain energy release rate, G_c) as a function of the proportion of mode II to mode I loading (defined as the phase angle, $\Psi = \tan^{-1}(K_{II}/K_I)$) are shown in Fig. 4a for the transverse orientation. It is clear that regardless of age, the fracture toughness of cortical bone in this breaking orientation is not lowest for pure mode I tensile loading; rather it is highest in mode I and progressively decreases, by a factor of four or more, as the shear contribution increases, i.e., with increasing phase angle. This is in stark contrast to the behavior of most materials, and indeed for cortical bone in the longitudinal orientation (Fig. 4b), where the toughness invariably increases with increasing phase angle. The critical G_c values reported in the longitudinal orientation (Fig. 4b) represent lower-bounds for the toughness as fracture invariably occurs at the loading pins in the direction of the weakest plane when using the asymmetric bending geometry in this orientation. However, the

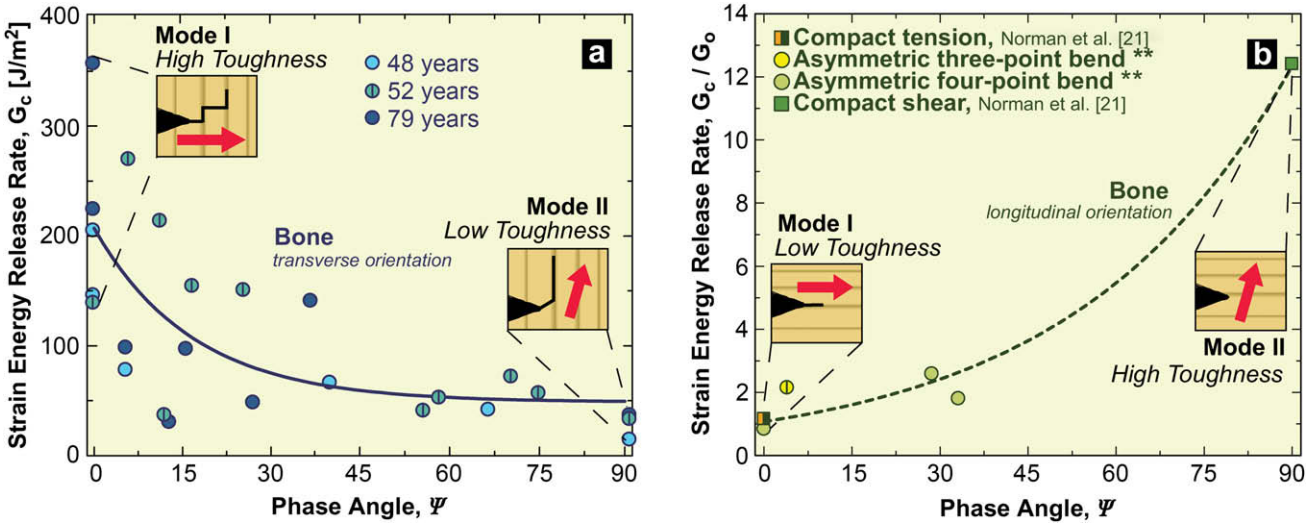

Fig. 4. The critical strain energy release rate, G_c, as a function of the phase angle, Ψ, is plotted for human cortical bone in the (a) transverse orientation and (b) the longitudinal orientation. The phase angle signifies the relative proportion of K_{II} to K_I; thus, for pure mode I tensile loading $\Psi = 0^\circ$, while for pure mode II shear loading $\Psi = 90^\circ$. While in the longitudinal orientation bone is strong in shear, the trend reverses in the transverse direction. This unique result sheds light on the strong influence of the microstructural orientation as compared to the applied mechanical driving force. In the insets, the faint brown lines indicate the direction of the weak microstructural planes, while the arrows indicate the direction of the maximum mechanical applied driving force (i.e., G_{max} or $K_{II} = 0$), which in mode I is coplanar with the original crack plane and in mode II is at about a 74° angle to the original crack plane [10]. Thus, a high toughness results when the driving force is perpendicular to the weak planes (transverse mode I and longitudinal mode II). As the preferred mechanical and microstructural directions get closer to alignment, the toughness correspondingly decreases. **The longitudinal data represent a lower-bound for the expected values and are compared to data from Norman et al. [21].

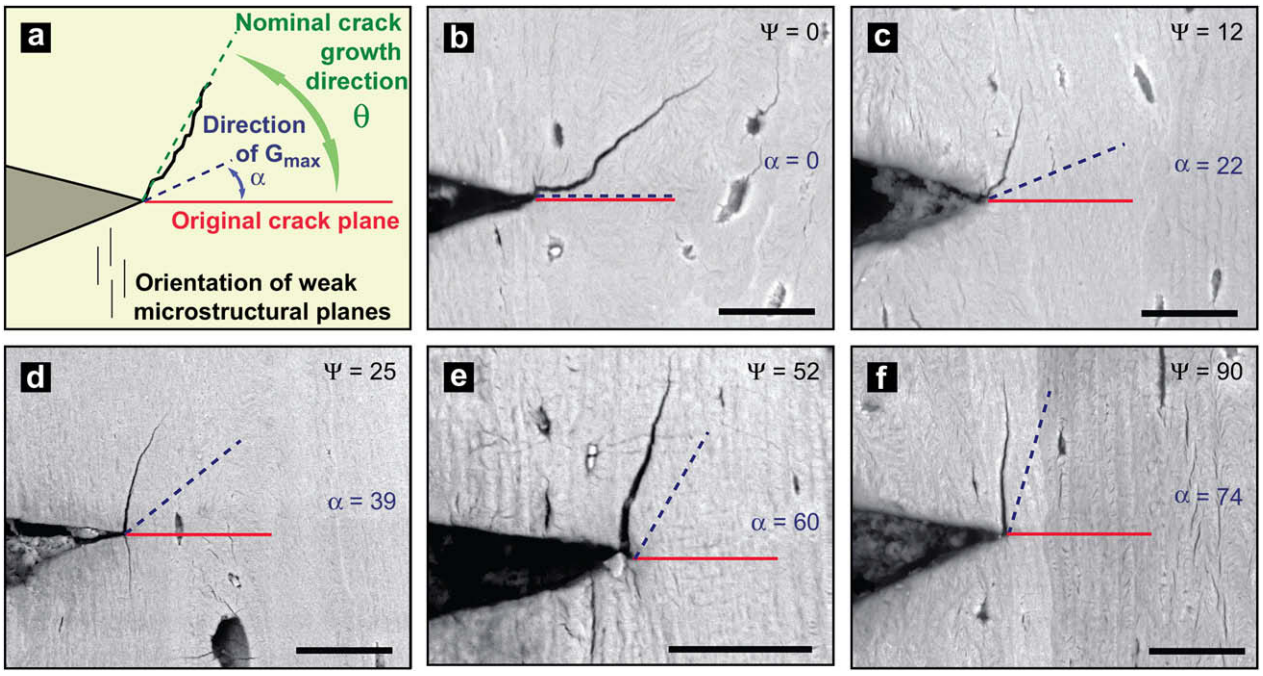

Fig. 5. Environmental scanning electron microscope (ESEM) backscattered-electron images of stable crack growth during *in situ* testing in the transverse orientations for phase angles of (b) $\Psi = 0°$, (c) $\Psi = 12°$, (d) $\Psi = 25°$, (e) $\Psi = 52°$ and (f) $\Psi = 90°$. (a) The crack growth angle, θ, (in green), with respect to the original crack plane (solid line in red), increases with the phase angle. The direction of maximum driving force (dashed line in blue) is also indicated and is defined here as the G_{max} path [10]. In (b–f), the scale bars are 50 μm.

longitudinal data matches fairly well with previously reported trends for human cortical bone in the same orientation, which were measured using the compact-tension and compact-shear test specimens [21]. Taken together, these results clearly indicate that in the transverse direction, human cortical bone is significantly less resistant to fracture in shear, with a mode II fracture toughness some 25% smaller than in mode I.

Typical environmental scanning electron micrographs of the initial trajectory of the crack, following crack initiation from the sharpened notch, are shown in Fig. 5 as a function of the phase angle. The crack can be seen to initially propagate at an increasing angle of deflection, θ, to the through-thickness plane of the notch as the proportion of shear loading increases, i.e., with increasing Ψ. Also indicated is the direction of maximum mechanical driving force, α, defined here as the path of maximum strain energy release rate, G_{max}; the values used were computed using the He and Hutchinson solution for a crack in a homogeneous material [10]. Fig. 6 illustrates the difference in the path of the maximum mechanical driving force and the actual path of crack growth in all of the transverse cortical bone samples. It is apparent that in general the crack does not follow this crack path with the deviation from this "expected" path highest at low phase angles. Such crack path deviations clearly indicate a marked influence of the microstructure, and its directionality, on the fracture process (Fig. 6).

The effects of mixed-mode loading on the through-thickness crack path in the transverse samples are clearly seen from scanning electron microscopy images of the fracture surfaces (Fig. 7) and X-ray computed tomographic images (Fig. 8). The fracture surface of a transverse sample loaded in pure mode I, $\Psi = 0°$ (Fig. 7a), has a torturous surface accounted for by crack deflection *on a scale of the order of hundreds of micrometers*, an effect which has been shown in previous studies to act as the dominant toughening mechanism [1]. Comparatively, in the sample loaded with a mode II driving force, $\Psi = 90°$ (Fig. 7b), gross crack deflection *on a scale on the order of millimeters* occurred but did not toughen the bone due to the fact that the directions of the maximum mechanical driving force and the "weakest" microstructural paths are nominally identical and both promote cracking in the same direction. Under such circumstances, resistance to fracture is low.

Three-dimensional synchrotron X-ray computed tomographic images of these bone samples further emphasize this difference in crack paths for low and high phase-angle loading and demonstrate the tortuous path of the deflected cracks in the transverse

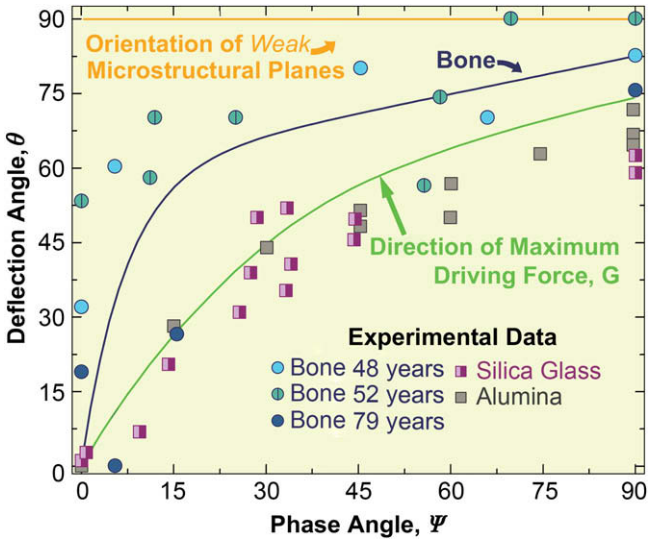

Fig. 6. Experimental crack deflection angle, θ, as a function of phase angle, Ψ, for human cortical bone in the transverse orientation, silica glass [30], and alumina [7]. The labeled green line indicates the predicted angle of deflection as a function of phase angle for a material following the maximum driving force condition, G_{max}, [10] while the labeled orange line indicates the position of the weak planes in this geometry. Traditional brittle materials follow the maximum driving force condition when a mixed-mode load is applied. However, in bone, application of a shear force in addition to the tensile force causes the direction of the driving force to change such that deflection along the weak microstructural planes becomes increasingly promoted.

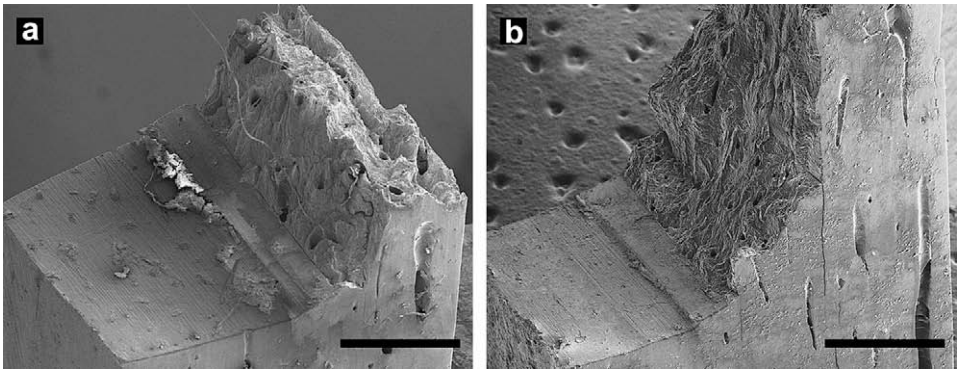

Fig. 7. SEM fractography images of human cortical bone after *in situ* testing in the transverse orientation for phase angles of (a) $\Psi = 0^\circ$, and (b) $\Psi = 90^\circ$. The mode I sample shows a torturous crack path due to the disparity between the orientation of the driving force and the weak microstructural path; this toughens the material. The mode II sample shows a macroscopic inclination of the crack, on the order of millimeters, which is promoted by the alignment of the driving force and the weak planes; this contributes little to the toughness of the material. In (a) and (b), the scale bars are 1 mm.

orientation where the preferred mechanical and microstructural crack paths are not coplanar (Fig. 8a). Indeed, the three-dimensionality of these images clearly indicates that cracks additionally deflect out-of-plane, i.e., they twist, which as shown in Ref. [1] is an even more potent mechanism of toughening than in-plane deflection.

5. Discussion

In materials without microstructural anisotropy, cracks tend to follow the path of maximum mechanical driving force, with a consequent increase in toughness from the lower-bound mode I value with increasing phase angle. Assuming a path of maximum strain energy release rate (essentially a $K_{II} = 0$ path), application of a pure mode I stress intensity will result in crack growth that is coplanar to the original crack plane, a pure mode II stress intensity will result in deflection at a 74° angle to this plane, and a mixed-mode (I + II) stress intensity will result in crack deflection at an angle between these limits of 0° and 74°. However, for nominally transverse (breaking) fractures, behavior in human cortical bone is completely different, with the toughness decreasing relative to the amount of shear loading, making the mode II toughness the lower-bound.

Such seemingly surprising behavior can be explained in terms of the competition between the paths of maximum mechanical driving force and microstructural "weakness". In human cortical bone, the longitudinal direction invariably represents the preferred microstructural path; microcracking occurs quite readily along the osteon boundaries (cement lines), which are orientated along the long axis of the bone. Considering first pure mode I conditions, if the bone is loaded in the longitudinal (splitting) orientation, the direction of the maximum driving force and microstructural

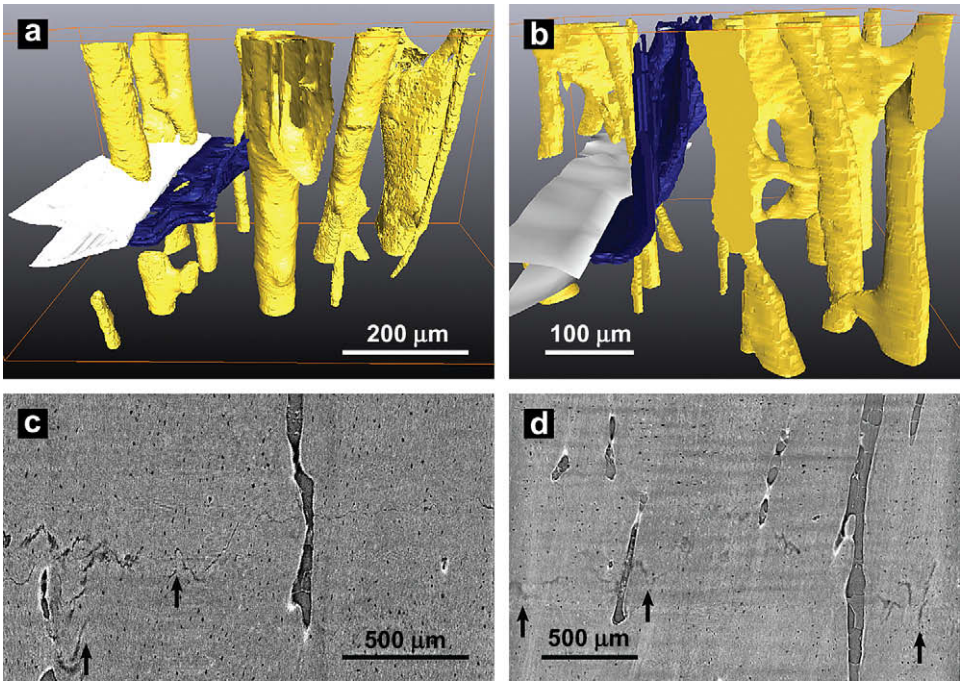

Fig. 8. Micro X-ray computed tomographic images of human cortical bone after *in situ* testing in the transverse orientation for phase angles of (a, c) $\Psi = 0^\circ$, and (b, d) $\Psi = 72^\circ$. In (a) and (b), the notch is colored white, the crack growth is in blue, and the Haversian canals are yellow. (a) The three-dimensional image of the mode I sample shows nominally straight crack growth with a deflection as the crack approaches the Haversian canal while the high phase-angle sample (b) shows one gross deflection of the crack to follow the preferred microstructural path along the cement lines. Images (c) and (d) are of the through-thickness crack profiles from the back-face of the sample, i.e., the crack is growing into the image. Both the high phase-angle sample and the mode I sample, exhibit crack bridging and twisting; regions of high twist are indicated by the black arrows in (c) and (d).

"weakness" coincide such that cracks propagate nominally in the expected longitudinal direction (see the inset of Fig. 4b); resulting fracture surfaces tend to be rather smooth and the toughness relatively low [1]. Conversely, for mode I loading in the transverse (breaking) orientation, these directions are orthogonal (as noted above); cracks are mechanically driven to propagate transversely to break the bone but on encountering the weak cement line interfaces are deflected longitudinally (see the inset of Fig. 4a). The fact that the preferred mechanical and microstructural paths are now incommensurate results in many deflections and twists in the crack trajectory, rough fracture surfaces and a much higher toughness – hence the observation that bone is easier to split than to break [1].

The same argument can be applied to explain behavior under mixed-mode conditions. As just described, when loaded in mode I in the transverse orientation, the preferred mechanical and microstructural paths are nominally orthogonal to each other, resulting in significant crack deflection and high toughness. Conversely, for pure mode II loading in the transverse orientation, the weakest microstructural direction remains longitudinal, i.e., at 90° to the crack plane, and is now more favorably oriented (within 20°) to the path of maximum driving force, which is at ~74° to the original crack plane (see the inset of Fig. 4a); this results in a single crack deflection and a corresponding lower toughness. Accordingly, for the transverse orientation, since reducing the phase angle from $\Psi = 90°$ to 0° (from pure mode II to pure mode I) results in an increasing divergence of the preferred mechanical and microstructural crack paths, the toughness is expected to increase at the lower phase angles, i.e., with a larger mode I component, due to the increased frequency and degree of crack deflection. In the mode I case, after the crack has deflected along the weak plane the driving force reorients the crack with respect to the direction of the maximum driving force. This allows the deflection process to occur many times and toughen the material. In this way, deflections only serve to toughen the material when the difference between the directions of the maximum mechanical driving force and weakest microstructural paths is large.

These results may be considered to have significant consequences as to how we view the relevance and applicability of fracture mechanics as applied to bone fracture. Undoubtedly, bones *in vivo* invariably fail under mixed-mode loading conditions yet virtually all assessments of the fracture resistance of bone have to date been performed in mode I, which we now know from the current work is clearly not the limiting condition. It would seem that for future characterizations of the failure of bone, it is imperative to include some degree of multiaxial loading as it is clear that cortical bone is far less resistant to shear (as compared to tensile) loading due to the marked directionality of its osteonal microstructure.

6. Conclusions

Based on an experimental study of the fracture mechanics of human cortical bone tested in 25 °C HBSS under mixed-mode loading conditions, i.e., in mode I (tensile) plus mode II (shear), the following conclusions can be made:

I. In the longitudinal (splitting) orientation, the fracture toughness of bone is lowest under pure mode I loading and increases with increasing phase angle (defined as the relative proportion of mode II to mode I stress intensities, $\Psi = \tan^{-1}(K_{II}/K_I)$). This is the characteristic behavior that is observed for many nominally brittle materials when loaded multiaxially in modes I and II.

II. In the transverse (breaking) orientation, the fracture toughness of bone is observed to display exactly the opposite behavior, in that the mode II fracture toughness is the lower-bound, with the toughness decreasing with increasing phase angle. Indeed, the mode II fracture toughness G_{IIc} is found to be ~25% or less than the mode I toughness G_{Ic}.

III. Such behavior is explained in terms of the competition between the direction of maximum crack-driving force, e.g., the path of maximum G or the $K_{II} = 0$ path, and the path of least microstructural resistance, which in bone is associated with the boundaries of the osteons (cement lines), which are nominally aligned longitudinally along the long axis of the bone. In the transverse orientation, when the mechanical and microstructural preferred paths are commensurate, crack paths tend to be inclined but without subsequent deflections, fracture surfaces are smooth and the toughness relatively low. Where these paths are incommensurate, increasing the divergence between the two paths causes many deflections and twisting of the crack, rough fracture surfaces and higher toughness.

IV. For fracture in the longitudinal (splitting) orientation, the mechanical and microstructural preferred paths are essentially coplanar in pure mode I such that the resultant fracture path is longitudinal with few crack deflections and the toughness is relatively low. Increasing the phase angle results in a progressively larger deviation between the mechanical and microstructural preferred paths that lead to more crack deflections and consequently higher toughnesses. In this orientation of bone, the lowest toughness is found for pure mode I loading, which is typical behavior for many materials.

V. For fracture in the transverse orientation, conversely, the mechanical and microstructural preferred paths are most closely aligned in mode II (i.e., shear loading), such that the mode II toughness is the lowest. Now decreasing the phase angle (the relative amount of shear to tensile loading) results in a progressively larger deviation between the mechanical and microstructural preferred paths, leading to more crack deflection and higher toughness. In this breaking orientation, the lowest toughness of cortical bone is found for pure mode II loading, which is unusual behavior for most materials.

Acknowledgements

This work was supported by the Laboratory Directed Research and Development Program of Lawrence Berkeley National Laboratory (LBNL), funded by the U.S. Department of Energy under contract no. DE–AC02–05CH11231. We acknowledge the use of the X-ray synchrotron micro-tomography beam line (8.3.2) at the Advanced Light Source at LBNL, supported by the Office of Science of the Department of Energy. The authors also wish to thank Professor Tony M. Keaveny and Mike Jekir, of the Mechanical Engineering Department at the University of California, Berkeley, for graciously allowing us to use their facilities to machine samples for this project.

Appendix

Figures with essential colour discrimination. Most figures in this article have features that may be difficult to interpret in black and white. The full colour images can be found in the on-line version, at doi:10.1016/j.biomaterials.2009.06.017.

References

[1] Koester KJ, Ager JW, Ritchie RO. The true toughness of human cortical bone measured with realistically short cracks. Nat Mater 2008;7(8):672–7.
[2] Nalla RK, Kruzic JJ, Kinney JH, Ritchie RO. Mechanistic aspects of fracture and R-curve behavior in human cortical bone. Biomaterials 2005;26(2):217–31.
[3] Norman TL, Vashishth D, Burr DB. Fracture toughness of human bone under tension. J Biomech 1995;28(3):309–20.
[4] Vashishth D. Rising crack-growth-resistance behavior in cortical bone: implications for toughness measurements. J Biomech 2004;37(6):943–6.

[5] Irwin GR. Analysis of stresses and strains near the end of a crack traversing a plate. J Appl Mech 1957;24:361–4.
[6] Qian J, Fatemi A. Mixed mode fatigue crack growth: a literature survey. Eng Fract Mech 1996;55(6):969–90.
[7] Singh D, Shetty DK. Fracture toughness of polycrystalline ceramics in combined mode I and mode II loading. J Am Ceram Soc 1989;72(1):78–84.
[8] Suresh S, Shih CF, Morrone A, O'Dowd NP. Mixed-mode fracture toughness of ceramic materials. J Am Ceram Soc 1990;73(5):1257–67.
[9] Melin S. When does a crack grow under mode II conditions? Int J Fract 1986;30(2):103–14.
[10] He M-Y, Hutchinson JW. Kinking of a crack out of an interface. J Appl Mech 1989;56:270–8.
[11] Wang J-S. Interfacial fracture toughness of a copper/alumina system and the effect of the loading phase angle. Mech Mater 1995;20(3):251–9.
[12] Evans AG, Hutchinson JW. Effects of non-planarity on the mixed mode fracture resistance of biomaterial interfaces. Acta Metall 1989;37(3):909–16.
[13] He MY, Cao HC, Evans AG. Mixed-mode fracture: the four-point shear specimen. Acta Metall Mater 1990;38(5):839–46.
[14] Ritchie RO, Cannon RM, Dalgleish BJ, Dauskardt RH, McNaney JM. Mechanics and mechanisms of crack growth at or near ceramic–metal interfaces: interface engineering strategies for promoting toughness. Mater Sci Eng A 1993;166(1–2):221–35.
[15] Martin RB, Burr DB. Structure, function, and adaptation of compact bone. New York: Raven Press; 1989.
[16] Currey JD. Bones: structure and mechanics. Princeton, NJ: Princeton University Press; 2002.
[17] Schaffler MB, Burr DB, Frederickson RG. Morphology of the osteonal cement line in human bone. Anat Rec 1987;217:223–8.
[18] Burr DB, Schaffler MB, Frederickson RG. Composition of the cement line and its possible mechanical role as a local interface in human compact bone. J Biomech 1988;21(11):939–41.
[19] Frasca P. Scanning-electron microscopy studies of 'ground substance' in cement lines, resting lines, hypercalcified rings and reversal lines of human cortical bone. Cells Tissues Organs 1981;109:115–21.
[20] Skedros JG, Holmes JL, Vajda EG, Bloebaum RD. Cement lines of secondary osteons in human bone are not mineral-deficient: new data in a historical perspective. Anat Rec A 2005;286A:781–803.
[21] Norman TL, Nivargikar SV, Burr DB. Resistance to crack growth in human cortical bone is greater in shear than in tension. J Biomech 1996;29(8):1023–31.
[22] Feng Z, Rho J, Han S, Ziv I. Orientation and loading condition dependence of fracture toughness in cortical bone. Mater Sci Eng C 2000;11(1):41–6.
[23] He M, Hutchinson JW. Asymmetric four-point crack specimen. J Appl Mech 2000;67(1):207–9.
[24] Tada H, Paris PC, Irwin GR. The stress analysis of cracks handbook. St. Louis, MO: Del Research Corp.; 1985.
[25] Anderson TL. Fracture mechanics: fundamentals and applications. 2nd ed. Boca Raton: CRC Press; 1995.
[26] Jen WK, Lin HC, Hua K. Calculation of stress intensity factors for combined mode bend specimens. In: Taplin DMR, editor. Fracture 1977: advances in research on the stress and fracture of materials/fourth international conference on fracture. Pergamon Press; 1977. p. 123–33.
[27] Kinney JH, Nichols MC. X-ray tomographic microscopy (XTM) using synchrotron radiation. Annu Rev Mater Sci 1992;22:121–52.
[28] Vlassenbroeck J, Dierick M, Masschaele B, Cnudde V, Van Hoorebeke L, Jacobs P. Software tools for quantification of X-ray microtomography at the UGCT. Nucl Instrum Methods Phys Res Sect A 2007;580:442–5.
[29] Jernkvist LO. Fracture of wood under mixed mode loading: II. Experimental investigation of Picea abies. Eng Fract Mech 2001;68(5):565–76.
[30] Li M, Sakai M. Mixed-mode fracture of ceramics in asymmetric four-point bending: effect of crack-face grain interlocking/bridging. J Am Ceram Soc 1996;79(10):2718–26.